Emerging Contaminants 12 (2026) 100620

Contents lists available at ScienceDirect

Emerging Contaminants

journal homepage: www.keaipublishing.com/en/journals/emerging-contaminants

Toxic effects of palmitoyl-, oleoyl-, and linoleoyl-fumonisin B1 derivatives on zebrafish embryos and their interactions with serum albumin

Zsolt Csenki [a,1], Illés Bock [a,1], Levente Horváth [b], Artur Stepniak [c], Béla Fiser [c,d,e], Adam Buczkowski [c], Gergő Tóth [f,g], Dávid Csabai [h], Dávid Hesszenberger [h], Anikó Lajtai [h], Sándor Kunsági-Máté [i,j], Melinda Kovács [k,l], István Szabó [a], Balázs Kriszt [m], Tibor Bartók [b], Miklós Poór [h,n,*]

[a] Department of Environmental Toxicology, Institute of Aquaculture and Environmental Safety, Hungarian University of Agriculture and Life Sciences, Páter Károly u. 1, H-2100, Gödöllő, Hungary
[b] Fumizol Ltd., Kisfaludy u. 6/B, H-6725, Szeged, Hungary
[c] Department of Physical Chemistry, Faculty of Chemistry, University of Lodz, Pomorska 163/165, Lodz, 90-236, Poland
[d] Higher Education and Industrial Cooperation Centre, University of Miskolc, H-3515, Miskolc-Egyetemváros, Hungary
[e] Rakoczi II Transcarpathian Hungarian College of Higher Education, 90200, Beregszász, Transcarpathia, Ukraine
[f] Department of Pharmaceutical Chemistry, Semmelweis University, H-1085, Budapest, Hungary
[g] Center for Pharmacology and Drug Research & Development, Semmelweis University, Üllői str. 28, 1085, Budapest, Hungary
[h] Department of Laboratory Medicine, Medical School, University of Pécs, Ifjúság útja 13, H-7624, Pécs, Hungary
[i] Department of Organic and Medicinal Chemistry, Faculty of Pharmacy, University of Pécs, Honvéd u. 1, H-7624, Pécs, Hungary
[j] Green Chemistry Research Group, János Szentágothai Research Centre, University of Pécs, Ifjúság útja 20, H-7624, Pécs, Hungary
[k] Institute of Physiology and Nutrition, Department of Physiology and Animal Health, Agribiotechnology and Precision Breeding for Food Security National Laboratory, Hungarian University of Agriculture and Life Sciences, H-2103, Gödöllő, Hungary
[l] HUN-REN-MATE Mycotoxins in the Food Chain Research Group, Hungarian University of Agriculture and Life Sciences, Guba Sándor u. 40, H-7400, Kaposvár, Hungary
[m] Department of Environmental Safety, Hungarian University of Agriculture and Life Sciences, Institute of Aquaculture and Environmental Safety, Páter Károly. u. 1, Páter Karoly u. 1, 2100 Gödöllő, Hungary
[n] Molecular Medicine Research Group, János Szentágothai Research Centre, University of Pécs, Ifjúság útja 20, H-7624, Pécs, Hungary

ARTICLE INFO

Article history:
Received 3 October 2025
Received in revised form
11 November 2025
Accepted 22 December 2025
Available online 23 December 2025

Keywords:
Fumonisin B1
Acyl-fumonisin B1 derivatives
Zebrafish
Toxicity
Human serum albumin

ABSTRACT

Acyl derivatives of the mycotoxin fumonisin B1 (FB1) occur in naturally infected grains and can be formed during certain food processing steps and/or as *in vivo* metabolites of the parent mycotoxin. The toxicity of *N*-acyl-FB1 metabolites is considerably higher compared to FB1; however, their toxic impacts and molecular interactions are barely characterized. To get a better insight into the structure-related and time-dependent toxic actions of acyl-FB1 derivatives, the effects of *N*-palmitoyl-, *N*-oleoyl-, *N*-linoleoyl-, 5-*O*-palmitoyl-, 5-*O*-oleoyl-, and 5-*O*-linoleoyl-FB1 were examined on zebrafish embryos. Furthermore, the interactions of these metabolites with human serum albumin (HSA) were investigated using fluorescence spectroscopy, isothermal titration calorimetry, and ultrafiltration. Our results underline the high *in vivo* toxicity of *N*-acyl-FB1 derivatives (LC_{50} = 4–18 μM; 120 h), followed by 5-*O*-acyl-FB1 (LC_{50} = 22–38 μM; 120 h) metabolites then FB1. Depending on the fatty acid component, the toxic potency and the time-dependent impacts showed large variations. *N*-palmitoyl-FB1 proved to be the most toxic derivative, causing high mortality at low micromolar levels even after 24 h exposure. Acyl-FB1 metabolites bind to HSA with high affinity ($\log K$ = 5.4–6.4), most of them occupy more binding sites on the protein. Interestingly, fatty acids, *N*-acyl-FB1 and 5-*O*-acyl-FB1 derivatives exerted different modulatory effects on the albumin binding of Site I and/or Site II markers examined. Our data demonstrate the similarities and differences regarding the toxic actions and the albumin binding

* Corresponding author. Department of Laboratory Medicine, Medical School, University of Pécs, Ifjúság útja 13, H-7624, Pécs, Hungary.
E-mail address: poor.miklos@pte.hu (M. Poór).
Peer review under the responsibility of KeAi Communications Co., Ltd.
[1] These authors contributed equally to this work.

https://doi.org/10.1016/j.emcon.2025.100620

properties of certain *N*-acyl- and 5-*O*-acyl-FB1 derivatives, and draw the attention to these barely examined mycotoxin metabolites.

1. Introduction

Mycotoxins are toxic secondary metabolites of filamentous fungal strains, they are undoubtedly among the most important food contaminants [1]. Fumonisin mycotoxins are mainly produced by *Fusarium* species, including *F. verticillioides* and *F. proliferatum* [2,3], but their formation has also been observed in certain black *Aspergillus* [4] and *Tolypocladium* [5] species. In terms of food safety, certain members of group FB appear to be the most important among the several fumonisin mycotoxins described [3]; therefore, an upper limit value for the sum of fumonisin B1 (FB1) and fumonisin B2 (FB2) toxins has been set in the EU (EU 2023/915). Due to the hepatocarcinogenic effect of FB1 observed in some animals and the increased incidence of human esophageal cancer accompanied with the high exposure to fumonisins [6], the International Agency for Research on Cancer (IARC) classifies FB1 as a possible human carcinogen (Group 2B) [7]. FB1 is a known inhibitor of ceramide synthase enzymes affecting sphingolipid biosynthesis, which seems to be a key mechanism of action regarding its toxic impacts [2,6,8]. In the recent decades, a number of masked/modified fumonisins have also been reported [9], including acylated fumonisin derivatives. The few data available underline the considerably higher toxicity of acyl-FB1 metabolites compared to the parent mycotoxin [10,11]. Therefore, further extensive studies are reasonable to examine the occurrence of acyl-FB1 derivatives in different foodstuffs, where the lack of reference materials causes a significant problem [12]. Few years ago, the *N*-palmitoyl-FB1 (*N*-pal-FB1) and 5-*O*-palmitoyl-FB1 (5-*O*-pal-FB1) derivatives were produced and purified (structures were confirmed by HRMS and NMR) [13]; and recently *N*-oleoyl-FB1 (*N*-ole-FB1), 5-*O*-oleoyl-FB1 (5-*O*-ole-FB1), *N*-linoleoyl-FB1 (*N*-lin-FB1), and 5-*O*-linoleoyl-FB1 (5-*O*-lin-FB1) were also prepared. These compounds provide an excellent opportunity for the more detailed investigations of acyl-FB1 derivatives, including their structure-related effects and interactions.

The formation of *N*-acyl-FB1 derivatives have been reported during the production tortilla chip (from FB1-contaminated maize): nixtamalization (soaking and cooking dried maize under alkaline conditions) then frying in preheated cooking oil [14]. Presumably, fatty acid anhydrides (produced by the heating of fats at high temperature) interact with FB1 [14]. Applying the tritium-labeled mycotoxin, an earlier study demonstrated the high production of *N*-acylated FB1 derivatives, where the following amounts were found compared to the initial FB1 levels: approximately 3 % and 2 % of free FB1 in tortilla chip and frying oil, respectively; while around 6 % and 80 % of *N*-acyl-FB1 derivatives in tortilla chip and frying oil, respectively [14]. These observations suggest that the repeated application of the oil used may cause higher accumulation of *N*-acyl-FB1 derivatives in tortilla chip. Furthermore, low amounts of *N*-acyl-FB1 (palmitoyl, oleoyl, and linoleoyl) metabolites were also found after solid-phase fermentation with toxigenic *F. verticillioides* strains in rice cultures [15]. Thus, certain fungal strains are able to synthesize these metabolites; however, based on our current knowledge, *N*-acyl-FB1 derivatives have never been detected as a result of natural field infection. Importantly, FB1 is partly biotransformed to its *N*-acyl derivatives in mammals [16]. This process is catalyzed by certain ceramide synthase isoforms [10,17,18], where FB1 is both inhibitor and substrate. After the i.p. administration of FB1 (0.5–2 mg/kg body weight) to rats, *N*-acyl-FB1 metabolites were detected in the liver and kidneys (approximately 0.2–0.4 nmol/g) of the animals [16]. In addition, after five days of repeated treatment (0.69–2.77 μmol FB1/kg body weight per day), the molar levels of *N*-acyl-FB1 metabolites in the liver were 0.1–0.3 % (in kidneys: <0.04 %) compared to the total dose of FB1 administered, which means circa 35–60 % of the total FB1 species found in the liver (in kidneys: <10 %) [16]. The considerably higher *in vitro* cytotoxicity of *N*-acyl-FB1 metabolites compared to the parent mycotoxin have been demonstrated on different cell lines [10]. Moreover, in zebrafish embryo model, *N*-pal-FB1 proved to be more toxic than FB1 based on both mortality data and sublethal malformations observed [11]. After 24 h exposure (at 120 hpf zebrafish embryos, treated in an exposure window of 96–120 hpf), even 6.25 μM concentration of *N*-pal-FB1 caused 100 % mortality while no FB1-induced mortality was noticed in the 0–200 μM range [11]. An earlier study demonstrated the high-affinity interaction of *N*-pal-FB1 with human serum albumin (HSA), where the results of ultracentrifugation and ultrafiltration experiments suggested that it may occupy more than one binding sites on the protein [11]. *N*-pal-FB1 considerably decreased the albumin-bound fractions of both Site II (naproxen) and Site I (warfarin) marker ligands, and modeling studies also identified these regions of HSA as the possible binding sites [11].

The presence of *O*-acyl-FB1 derivatives (or also known as esterified fumonisins) were first demonstrated in rice cultures inoculated with *F. verticillioides*, where the total amount of palmitoyl-, oleoyl-, and linoleoyl-FB1 compounds identified comprised approximately 0.1 % of the FB1 concentration [19]. Oleoyl and linoleoyl metabolites have also been identified in naturally infected maize (typically 5–7 % together compared to the FB1 levels) [20]. In addition, after 45 days incubation of *F. verticillioides* in cornmeal media and rice-based media, the total amounts of *O*-acyl derivatives were 0.7–3.5 % and 0.0–2.9 % compared to the concentrations of FB1, respectively [21]. After 24 h treatment of zebrafish embryos, 5-*O*-pal-FB1 did not cause mortality at 50 μM or lower levels; however, approximately 10 % and 30 % mortality was observed in the presence of its higher concentrations (100 μM and 200 μM, respectively) [11]. The comparison with *N*-pal-FB1 and FB1 highlighted that 5-*O*-pal-FB1 is less toxic than the *N*-palmitoyl derivative and more toxic compared to FB1, which conclusion was also supported by the evaluation of the mycotoxin-induced sublethal malformations [11]. Similar to the *N*-palmitoyl metabolite, 5-*O*-pal-FB1 also showed strong interaction with HSA; however, it decreased only the albumin-bound fraction of the Site I marker warfarin, while Site II was not affected [11]. Nevertheless, the binding constants and the number of binding sites regarding acyl-FB1–HSA interactions remained unclear.

Although, only limited information is available, the above-listed data emphasize the potential toxicological importance of acyl-FB1 derivatives, including their toxic impacts and toxicokinetics. To get a deeper insight into the structure-related and time-dependent harmful effects of acyl-FB1 metabolites, in the current study, the mycotoxin-induced mortality was tested after 24, 48, 72, 96, and 120 h exposure, then the sublethal malformations were also

evaluated for FB1, *N*-pal-FB1, *N*-ole-FB1, *N*-lin-FB1, 5-*O*-pal-FB1, 5-*O*-ole-FB1, and 5-*O*-lin-FB1 (Fig. S1). In addition, to provide quantitative data for acyl-FB1–HSA interactions and to see the potential structure-dependent differences in their albumin binding, fluorescence spectroscopic, isothermal titration calorimetry, and ultrafiltration studies were applied.

2. Materials and methods

2.1. Materials

FB1 and acyl-FB1 derivatives were prepared and purified as it has been reported [13]. Briefly, acylation of FB1 toxin was carried out in tetrahydrofuran (THF) in the presence of triethylamine and the corresponding acyl chloride. When the acylation was performed in anhydrous THF, only *N*-acyl derivatives were formed rapidly; while in THF containing 2 v/v% water, 5-*O*-acyl FB1 toxins were obtained during 10 days. The reaction mixtures were evaporated to dryness, redissolved in acetonitrile/water (80/20, v/v), filtered through nylon syringe filters, and finally purified by preparative HPLC on a Kinetex C18 column (250 × 21.2 mm, 5 μm; Phenomenex, Torrance, CA, USA). The purity of *N*-pal-FB1 (≥99.0 %), *N*-ole-FB1 (≥95.4 %), *N*-lin-FB1 (≥97.2 %), 5-*O*-pal-FB1 (≥99.0 %), 5-*O*-ole-FB1 (≥98.6 %), and 5-*O*-lin-FB1 (≥95.2 %) were determined with HPLC–MS in full scan mode (150–1100 *m/z*). HSA (product code: A1653), naproxen, and racemic warfarin were obtained from Merck (Darmstadt, Germany). HPLC–UV grade acetonitrile, methanol, and water were purchased from Fisher Chemical (Fisher Scientific Company L.L.C., Pittsburgh, PA, USA). Mycotoxin–HSA interactions were examined in phosphate-buffered saline (PBS; 137 mM NaCl, 2.7 mM KCl, 10 mM Na_2HPO_4, and 1.8 mM KH_2PO_4 in water; pH 7.4).

2.2. Zebrafish

Laboratory bred AB zebrafish line was maintained in breeding groups of 30 females and 30 males at the Department of Environmental Toxicology (Hungarian University of Agriculture and Life Sciences, Gödöllő, Hungary). The fish were housed in a Tecniplast ZebTEC recirculation system (Tecniplast S.p.a., Buguggiate, Italy) under controlled conditions: 25.5 ± 0.5 °C, pH 7.0 ± 0.2, and conductivity 550 ± 50 μS, with a 14 h:10 h light:dark photoperiod. They were fed twice daily with dry granulated feed (Gemma Wean 500, Skretting, Norway), and additionally received freshly hatched *Artemia salina* twice per week. For spawning, adult zebrafish were placed in breeding tanks (Tecniplast S.p.a.) the evening before the experiment, and spawning was initiated by removing the divider the following morning. Eggs were collected and incubated in Petri dishes (diameter: 10 cm) filled with sterile E3 medium (5.0 mM NaCl, 0.17 mM KCl, 0.33 mM $CaCl_2$, and 0.33 mM $MgSO_4$ in 1 L sterilized distilled water). Embryos at the four-to eight-cell stage showing normal development were selected.

The exposure of the zebrafish embryos was carried out according to the Zebrafish Emrbryo Toxicity Assay (ZETA) [22]. Briefly, embryos were placed in 24-well tissue-culture plates in groups of five in four replicates ($n = 20$). Considering the results of our previous study with FB1, *N*-pal-FB1, and 5-*O*-pal-FB1 [11], the embryos were exposed to the following concentrations of each tested compound: 100 μM, 50 μM, 25 μM, 12.5 μM, 6.25 μM, 3.13 μM, 1.56 μM, 0.78 μM, and 0.39 μM. The exposure solutions were diluted from DMSO stock solutions using sterile E3 medium. Negative controls of E3 medium and DMSO solution – according to the highest concentration of the solvent in the exposure media – were also tested in four replicates. The plates were kept in an incubator at 25.5 ± 0.5 °C for 120 h, and mortalities were recorded daily.

After 120 h, surviving embryos from each group were anaesthetized with 100 mg/L MS-222 (tricaine methanesulfonate) solution, and placed in 4 % methylcellulose for photography. Bright field (exposure time: 6 msec, magnification: 30 ×) images of the embryos were taken under a stereomicroscope (Leica M205 FA stereomicroscope, Leica DFC 7000 T camera, Leica Application Suite X, Leica Microsystems GmbH; Wetzlar, Germany).

From the mortality rates, LC_{50} values and 95 % confidence intervals for all chemicals at each time point were primarily calculated using linear interpolation and bootstrapping ($n = 1000$). Where applicable, LC_{50} values were derived using a four-parameter logistic (4 PL) curve fit. Dose-response curves were drawn using cumulative Gaussian non-linear regression model (Graphpad Prism 8, GraphPad Software; San Diego, CA, USA). Sublethal defects were quantified by visual scoring of images of surviving embryos from the two selected treatment groups (3.13 μM and/or 25 μM). The frequencies of representative developmental defects are given as mean appearance (% ± SD). Potential significant differences across treatment groups at each defect were analyzed using two-way ANOVA with Tukey's post-hoc multiple comparisons test ($p < 0.05$).

2.3. Fluorescence spectroscopic studies

Fluorescence spectroscopic measurements were performed applying a Hitachi F-4500 fluorescence spectrophotometer (Tokyo, Japan). Emission spectra were recorded at 25 °C in 1 cm × 1 cm cuvettes, using 295 nm excitation wavelength with 90-degree fluorescence detection. Samples contained standard level of HSA (2 μM) and increasing concentrations of mycotoxins (0–20 μM) in PBS (pH 7.4). The ligand-induced increases in the emission signal of the protein were evaluated at 329 nm for *N*-acyl-FB1 metabolites and at 327 nm for 5-*O*-acyl-FB1 derivatives.

Non-linear parameter fitting method implemented in the HypSpec 2014 code (Protonic Software, Leeds, GB) is applied to determine the binding constants (*K*; unit: L/mol) of mycotoxin (M) – serum albumin (A) complexes as follows:

$$pA + qM \leftrightarrow A_pM_q \tag{1}$$

$$\beta_{pq} = \frac{[A_pM_q]}{[SA]^p[MT]^q} \tag{2}$$

where β reflects the overall binding constants, while p and q denote the coefficients which indicate the stoichiometry associated with the equilibrium.

$$A + M \leftrightarrow A\,M \quad \beta_1 = \frac{[A\,M]}{[A][M]} \tag{3}$$

$$A + qM \leftrightarrow A\,M_q \quad \beta_q = \frac{[A\,M_q]}{[A][M]^q} \tag{4}$$

The relationship between the overall binding constants and the stepwise binding constants is known as the followings.

$$\beta_1 = K_1;\ \ \beta_q = K_1 \times K_2 \ldots \times K_q \tag{5}$$

The stoichiometry and binding constants of mycotoxin-albumin complexes were determined by the model associated with the lowest standard deviation. As mathematical aspect, the fitting algorithm focused on logβ, so in this HypSpec 2014 code the logβ is refined rather than the equilibrium constant β. This method makes the fitting procedure more stable and go somewhat faster since automatically excludes the negative values of the equilibrium constants from the proper solution of the equations above.

During the fitting procedure we considered that both the albumin and slightly the mycotoxin contribute to the formation of spectroscopic signal. However, while the contribution of the albumin in the absence of the mycotoxin is known as its molar absorptivity, the contributions of both the mycotoxin and albumin in the presence of the mycotoxin is unknown in the HypSpec model (and therefore calculated during the fitting procedure).

2.4. Isothermal titration calorimetry

Using isothermal titration calorimetry (VP-ITC calorimeter, MicroCal) the heat effects of titration of 5 μM HSA protein solutions with 260 μM solution of each of the following mycotoxins (*N*-pal-FB1, 5-*O*-pal-FB1, *N*-ole-FB1, 5-*O*-ole-FB1, *N*-lin-FB1, and 5-*O*-lin-FB1) were measured in aqueous 10 v/v% DMSO solution (used as solvent) at 25 °C. HSA solution with volume 1427.5 μL (in the working cell) was titrated with adding 5 μL aliquots (from the syringe) in total 275 μL volume of each mycotoxin solution. The reference cell was filled with aqueous 10 v/v% DMSO. The time during each injection was 10 s and the time between successive injections was 1000 s. The stirring speed was 307 rpm. Independently the heat effects of each mycotoxin dilution (from the syringe) into the solvent (in the cell) were measured maintaining the same parameters as during the proper titration.

Heat effects of direct interactions of HSA with each mycotoxin were calculated by subtracting the heat effects of mycotoxin dilution from the heat effects of HSA with mycotoxin titration. Obtained isotherms were next fitted with non-linear multiparameter regression method (Origin 7.0 MicroCal) using One Set of Sites model (ITC Date Analysis in Origin - Tutorial Guide. Northampton: MicroCal, 2004) to obtain the binding parameters: stoichiometry (n; describing the number of binding sites in the protein), binding/association constant (K; unit: L/mol) of each ligand with the active site of protein, and standard thermodynamic functions (including enthalpy (ΔH), entropy (ΔS), and Gibbs free energy of binding (ΔG)).

2.5. Ultrafiltration experiments

Ultrafiltration experiments were performed as it has been earlier reported [23,24]. Briefly, Amicon Ultra-0.5 centrifugal filters (30 kDa molecular weight cut-off; Merck, Darmstadt, Germany) were washed with 500 μL of water then with 500 μL of PBS (pH 7.4). In the Site I assay, warfarin (1.0 μM) and HSA (5.0 μM) were centrifuged (10 min, 7500 g, 25 °C; fixed angle rotor) without and with the ligands examined (10 or 20 μM) in PBS. In the Site II assay, naproxen (1.0 μM) and HSA (1.5 μM) were centrifuged (10 min, 7500 g, 25 °C; fixed angle rotor) in the absence and the presence of the ligands examined (10 or 20 μM) in PBS. We applied different albumin concentrations in the two assays because we aimed to achieve approximately 50 % albumin-induced decreases in site marker levels of the filtrate. After ultrafiltration experiments, concentrations of warfarin and naproxen were directly analyzed from the filtrates with UHPLC–FLD and HPLC–UV, respectively.

Warfarin was quantified in the filtrates with a Shimadzu UHPLC–FLD system (Kyoto, Japan), a degasser (DGU-20A5R), built up from an autosampler (Nexera X2 SIL-30AC), the pump modules (Nexera X2 LC30AD), a column oven (CTO-20AC), a fluorescence detector (RF-20A XS), and the LabSolutions 5.97 SP1 software. Samples (20 μL) were driven through a precolumn (SecurityGuard EVO-C18 ULTRA; Phenomenex) linked to a Kinetex EVO C18 analytical column (150 × 4.6 mm, 2.6 μm particle size, pore size 100 Å; Phenomenex), where the isocratic elution was performed with sodium phosphate buffer (20 mM, pH 7.0), methanol, and acetonitrile (70:25:5 v/v%) mobile phase, with 1.0 mL/min flow rate (column temperature: 24 °C). The total running time for each sample was 15 min, warfarin was detected at 390 nm (λ_{ex} = 310 nm).

Naproxen was quantified in the filtrates with an integrated HPLC–UV system (Jasco, Tokyo, Japan), containing an autosampler (AS-4050), a binary pump (PU-4180), an UV detector (UV-975), and the ChromNAV2 software, applying the previously reported method [25,26]. Briefly, samples (20 μL) were driven through a precolumn (SecurityGuard C18; Phenomenex) linked to a Gemini C18 analytical column (150 × 4.6 mm, 3 μm; Phenomenex). The isocratic elution was carried out using sodium acetate buffer (6.9 mM, pH 4.0) and acetonitrile (50:50 v/v%) as the mobile phase, with a 1 mL/min flow rate at room temperature. Naproxen was detected at 230 nm.

3. Results and discussion

3.1. Time-dependent mortality caused by FB1 and acyl-FB1 derivatives on zebrafish embryos

The toxicity of FB1 and its acyl metabolites (0–100 μM each) were tested on zebrafish embryos after 24, 48, 72, 96, and 120 h exposure. FB1 did not cause significant mortality at the concentration range tested (Fig. S2–S5 and Fig. 1A); therefore, no LC_{50} values were determined for the parent mycotoxin. This is in agreement with our previous results [11] as well as with the earlier findings of du Plessis et al. [27], where also the low acute toxicity of FB1 have been reported in zebrafish embryos. Furthermore, in the untreated and the solvent control groups, no mortality was observed.

Fig. 1A demonstrates the concentration–mortality curves of mycotoxins after 5 days of exposure. Generally, *N*-acyl-FB1 derivatives proved to be more toxic than *O*-acyl compounds. After 120 h exposure, the most potent toxicity was induced by *N*-pal-FB1 ($LC_{50} \approx 4$ μM), followed by *N*-ole-FB1 ($LC_{50} \approx 5$ μM) then *N*-lin-FB1 ($LC_{50} \approx 18$ μM). Interestingly, among the *O*-acyl metabolites, 5-*O*-ole-FB1 was the most toxic at 120 hpf ($LC_{50} \approx 22$ μM), followed by 5-*O*-lin-FB1 ($LC_{50} \approx 36$ μM) and 5-*O*-pal-FB1 ($LC_{50} \approx 38$ μM).

Another important issue is the time-dependence of the mycotoxin-induced mortality. The strong toxic effect of *N*-pal-FB1 has been developed during the first day of exposure ($LC_{50} \approx 8$ μM; Fig. S2); thereafter, the LC_{50} values were only moderately decreased over the next four days (Fig. 1B and Table S1). However, after 24 hpf, less potent impacts were noticed for *N*-ole-FB1 ($LC_{50} \approx 49$ μM) and *N*-lin-FB1 ($LC_{50} \approx 79$ μM), then their LC_{50} values were gradually decreased day by day (Fig. 1B and Table S1). After 5 days of exposure, *N*-ole-FB1 became similarly toxic to *N*-pal-FB1. Interestingly, 5-*O*-pal-FB1 and 5-*O*-ole-FB1 caused high mortality only at 96 hpf and 120 hpf. In contrast, the treatment with 5-*O*-lin-FB1 led to relevant mortality even after 48 h, then its toxic potency gradually increased over the following three days (Fig. 1B and Table S1). Furthermore, at 72 hpf and 96 hpf, 5-*O*-lin-FB1 showed similar concentration–mortality curves than *N*-lin-FB1 (Fig. S4 and S5). As another interesting observation, at 96 hpf, 5-*O*-lin-FB1 and 5-*O*-pal-FB1 induced higher mortality compared to 5-*O*-ole-FB1 (Fig. S5), and the latter metabolite became the most toxic among the *O*-acyl derivatives only after 120 h (Fig. 1B and Table S1). Based on these data, the site of acylation (*N*-acyl or 5-*O*-acyl) has a major importance; however, the structure of the fatty acid component is also a relevant factor in the toxicity of acyl-FB1 derivatives.

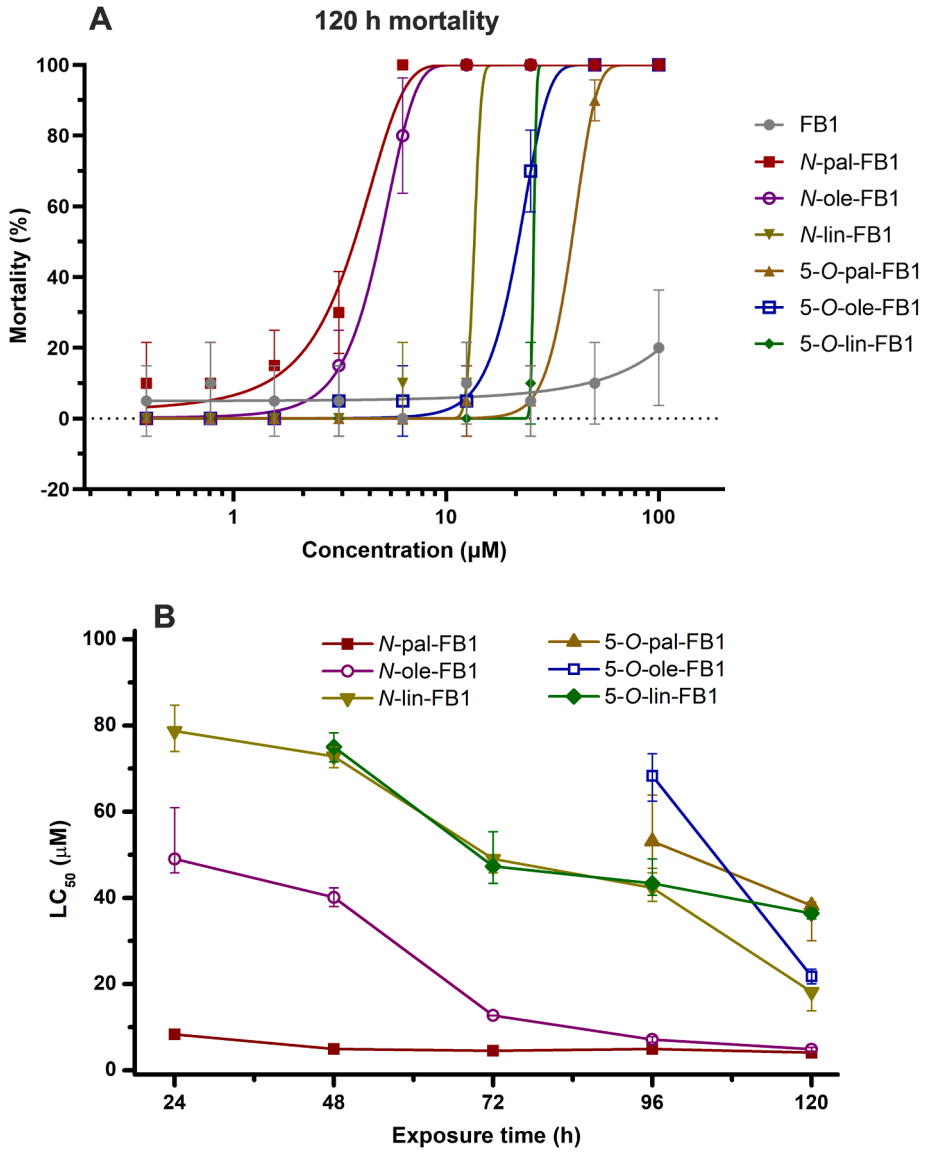

Fig. 1. Concentration–mortality curves of FB1 as well as its *N*-acyl and 5-*O*-acyl derivates after 120 h exposure in zebrafish embryos (120 hpf; $n = 20$ in each treatment group; **A**). LC_{50} values ± the range of the confidence intervals (CI) determined for acyl-FB1 derivatives at each time point (24, 48, 72, 96, and 120 h; see data in Table S1), where the values were primarily calculated using linear interpolation and bootstrapping ($n = 1000$; **B**).

3.2. Sublethal toxic effects of FB1 and acyl-FB1 derivatives on zebrafish embryos

In addition to mortality, sublethal malformations were also evaluated from the images of the surviving individuals from each test group (Fig. 2). We selected the 3.13 μM groups for phenotypic studies, since after the treatment with this concentration, an appreciable number of the embryos survived at the end of the test period (120 hpf). Because of their lower toxicity, the evaluation was also performed on the surviving individuals at 25 μM concentrations for FB1 and its 5-*O*-acyl derivates (Table 1). Generally, the uninflated swim bladder was a common symptom that was induced by all substances tested, which frequently occurs in zebrafish embryos after the exposure to various compounds as an indicator of developmental toxicity, particularly with chemicals that affect the development of circulation and/or osmoregulatory processes [28]. Regarding FB1 (at both 3.13 μM and 25 μM) and 5-*O*-acyl derivatives (treated with 3.13 μM), it was the only characteristic malformation in the surviving embryos. In zebrafish embryos treated with *N*-acyl-FB1 derivates (3.13 μM), the malformations in the head region (mainly the deformity of the lower jaw and the olfactory region) occurred with high frequency. These symptoms, along with pericardial edema, were only induced by the 25 μM concentrations of 5-*O*-acyl metabolites. Craniofacial lesions are much more specific symptoms than swim bladder malformations, which have been observed in several species besides zebrafish following their treatment with fumonisin-type mycotoxins [29,30]. Yolk lesions and discoloration were caused by *N*-pal-FB1 and *N*-ole-FB1 (3.13 μM), and by the higher concentrations (25 μM) of 5-*O*-acyl derivates.

The zebrafish embryo serves as a widely utilized vertebrate model for investigating the toxicity of various xenobiotics [31,32], including mycotoxins [33,34]. Due to their external fertilization and transparent nature, these embryos allow straightforward visual assessments, making them valuable for the *in vivo* detection of xenobiotic-induced lethality, toxicity, and developmental defects

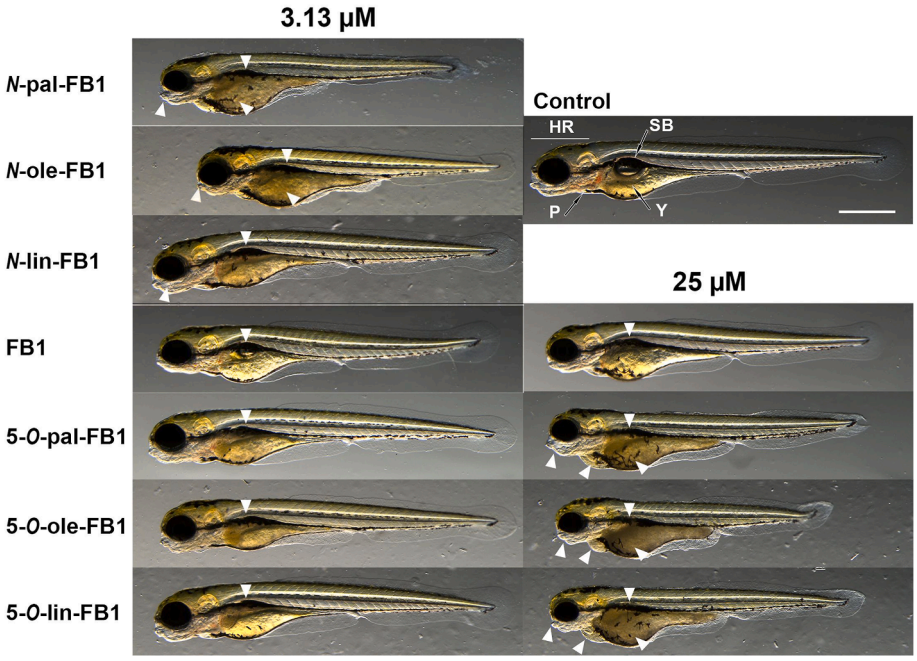

Fig. 2. Sublethal effects of FB1 and its *N*-acyl and 5-*O*-acyl derivates after 120 h treatment of zebrafish embryos. Representative phenotype lesions are indicated by arrows (P, pericardium; SB, swim bladder; Y, yolk; HR, head region). The scale bar indicates 500 μm.

at different larval stages [35,36]. Additionally, the embryonic development of zebrafish closely resembles that of higher vertebrates [37].

Mortality data underlined the more potent toxic impacts of *N*-acyl-FB1 derivatives vs. FB1 and even compared to 5-*O*-acyl compounds. In accordance with mortality, the sublethal effects also suggest the following order of toxicity: *N*-pal-FB1 > *N*-ole-FB1 > *N*-lin-FB1 > 5-*O*-ole-FB1 > 5-*O*-lin-FB1 > 5-*O*-pal-FB1 > FB1. Among the sublethal symptoms, the uninflated swim bladder was a common impact, affecting a significant portion of the surviving embryos even at low micromolar concentrations. It can be considered as a general symptom after the exposure to FB1 and its *N*-acyl and 5-*O*-acyl derivates, with its development even after a short exposure [11].

Previous *in vivo* studies suggest that liver and kidneys are major target organs of FB1 in certain animal species [38]. Hepatotoxic effects and metabolic disorders, primarily lipid metabolism disorders [39,40], in zebrafish embryos often cause changes in the yolk of individuals (different coloration, yolk retention, etc.) [39], which we observed in zebrafish embryos treated with high concentrations of 5-*O*-acyl derivates and with low micromolar levels of *N*-acyl compounds. Regarding the 5-*O*-acyl-FB1 metabolites (25 μM), yolk malformations were typically accompanied with the appearance of pericardial edema (Table 1). Given the essential role of the kidney in osmoregulation, if a toxic compound causes developmental abnormalities of the pronephros in zebrafish embryos, then it can often be the cause of the abnormal development of yolk or pericardial edema [41]. Since no pericardial edema or changes were found in the yolk of individuals treated with FB1, these observations may indicate a higher hepatotoxic and nephrotoxic potential of acyl-FB1 derivates compared to the parent mycotoxin.

FB1 is a relatively hydrophilic compound with limited transport through the cell membranes by passive diffusion, as it has been demonstrated by its poor absorption and bioavailability in *in vitro* and *in vivo* studies [2]. However, the fatty acid components of acyl-FB1 derivatives considerably increase their lipophilicity and diffusibility compared to the parent mycotoxin. Therefore, it is reasonable to hypothesize that the markedly higher toxic potency of acyl-FB1 metabolites vs. FB1 is at least partly resulted from their better diffusibility and more effective cellular/tissue uptake. The order of their elution from the C18 column [11] during our LC–MS analysis (see the retention times – t_R – in parentheses) indicates that *N*-ole-FB1 (t_R = 12.0 min) is the most lipophilic, followed by *N*-pal-FB1 (t_R = 11.7 min), *N*-lin-FB1 (t_R = 11.1 min), 5-*O*-ole-FB1 (t_R = 10.3 min), 5-*O*-pal-FB1 (t_R = 10.1 min), and finally 5-*O*-lin-FB1 (t_R = 9.6 min). On one hand, it is in agreement with the observation that *N*-acyl derivatives are more toxic compared to the *O*-acyl metabolites. On the other hand, we cannot see a clear correlation between the lipophilicity and the toxicity of acyl-FB1 compounds. In addition, the toxic mechanism of acyl-FB1 metabolites has not been characterized yet; therefore, the potential involvement of toxicodynamic reason(s)/component(s) cannot be ruled out.

3.3. Interactions of acyl-FB1 derivatives with HSA based on fluorescence spectroscopic studies

In these experiments, the impacts of acyl-FB1 compounds on the fluorescence emission signal of HSA were examined. Therefore, increasing concentrations of mycotoxins were added to standard level of the protein, after which emission spectra were recorded. Using 295 nm excitation wavelength, HSA showed its emission maximum around 340 nm. In the presence of each acyl-FB1 metabolite, the fluorescence signal of the protein increased, and a blue shift in its emission wavelength maximum was noticed (Fig. 3). When the *N*-acyl derivatives were added, we observed approximately 1.8-fold elevations in the emission intensity and the emission wavelength maxima moved to 329 nm (Fig. 3A, B, and C). However, *O*-acyl metabolites induced lower (circa 1.2-fold) increases in the emission signal and changed the final emission wavelength maxima to 327 nm (Fig. 3D, E, and F). The emission spectra did not show further relevant changes above 15 μM and 7 μM concentrations of *N*-acyl-FB1 and *O*-acyl-FB1, respectively.

Table 1
The mean appearance (% ± SD) of representative developmental defects among surviving embryos after the exposure (120 h) to FB1 and its *N*-acyl and 5-*O*-acyl derivates (pe, pericardial edema; usb, uninflated swim bladder; sbl, shortened body length; hd, head deformity; iay, improper absorption of yolk). Number of surviving embryos (out of $n = 20$) is indicated for each treatment in parenthesis. Superscript letters demonstrate the statistically significant differences based on two-way ANOVA with Tukey's post-hoc multiple comparisons test ($p < 0.05$), where the groups sharing a letter are not different (per defect, across treatments).

		FB1		*N*-pal-FB1	*N*-ole-FB1	*N*-lin-FB1	5-*O*-pal-FB1		5-*O*-ole-FB1		5-*O*-lin-FB1	
		3.13 μM ($n = 19$)	25 μM ($n = 19$)	3.13 μM ($n = 14$)	3.13 μM ($n = 17$)	3.13 μM ($n = 20$)	3.13 μM ($n = 20$)	25 μM ($n = 19$)	3.13 μM ($n = 19$)	25 μM ($n = 6$)	3.13 μM ($n = 20$)	25 μM ($n = 18$)
Freq. (%)	**pe**	0.0^{a} (±0.0)	0.0^{a} (±0.0)	12.5^{ab} (±14.4)	17.5^{ab} (±11.9)	30.0^{bc} (±11.5)	30.0^{bc} (±11.5)	50.0^{c} (±11.5)	15.0^{bc} (±10.0)	75.0^{d} (±28.9)	30.0^{bc} (±11.5)	100.0^{d} (±0.0)
	usb	80.0^{ab} (±16.3)	100.0^{b} (±0.0)	100.0^{b} (±0.0)	100.0^{b} (±0.0)	80.0^{ab} (±16.3)	80.0^{ab} (±16.3)	100.0^{b} (±0.0)	100.0^{b} (±0.0)	100.0^{b} (±0.0)	70.0^{a} (±11.5)	100.0^{b} (±0.0)
	sbl	0.0^{a} (±0.0)	0.0^{a} (±0.0)	70.8^{c} (±4.8)	45.0^{b} (±10.0)	0.0^{a} (±0.0)	0.0^{a} (±0.0)	80.0^{cd} (±16.3)	26.3^{ab} (±9.5)	100.0^{d} (±0.0)	5.0^{a} (±10.0)	100.0^{d} (±0.0)
	hd	0.0^{a} (±0.0)	10.0^{ab} (±11.5)	58.3^{c} (±9.6)	45.0^{bc} (±19.1)	30.0^{b} (±20.0)	30.0^{b} (±20.0)	57.5^{c} (±5.0)	26.3^{ab} (±9.5)	75.0^{cd} (±28.9)	5.0^{a} (±10.0)	100.0^{d} (±0.0)
	iay	0.0^{a} (±0.0)	30.0^{b} (±11.5)	100.0^{d} (±0.0)	55.0^{c} (±10.0)	5.0^{a} (±10.0)	5.0^{a} (±10.0)	95.0^{d} (±10.0)	26.3^{ab} (±9.5)	75.0^{cd} (±28.9)	0.0^{a} (±0.0)	100.0^{d} (±0.0)

Furthermore, we noticed saturation type concentration–intensity curves reaching their plateaus around 15–20 μM for *N*-acyl compounds (λ_{em} = 329 nm; Figs. 3G) and 7–10 μM for *O*-acyl derivatives (λ_{em} = 327 nm; Fig. 3H). Based on these data, the binding constants were determined with non-linear fitting, applying the HypSpec software (see details in Section 2.3). Importantly, acyl-FB1 derivatives did not show any background fluorescence in the absence of HSA, and they had no absorption at the excitation and emission wavelengths used. Even if the stoichiometry of these mycotoxin–HSA complexes were unclear at this point, we found a good fitting with the 1:1 stoichiometry model, suggesting the formation of more stable complexes of *O*-acyl-FB1 metabolites ($\log K = 6.12 \pm 0.16$ for 5-*O*-pal-FB1, 6.14 ± 0.25 for 5-*O*-ole-FB1, and 5.94 ± 0.09 for 5-*O*-lin-FB1) with the protein compared to the *N*-acyl-FB1 derivatives ($\log K = 5.40 \pm 0.08$ for *N*-pal-FB1, 5.51 ± 0.11 for *N*-ole-FB1, and 5.52 ± 0.18 for *N*-lin-FB1).

Typically, the complex formation of a ligand with HSA leads to a partial decrease in the emission signal of the protein, which is the basis of fluorescence quenching studies [42]. In contrast, in our previous [11] and current studies, the emission signal of the protein was increased by few micromolar levels of acyl-FB1 metabolites (Fig. 3) and by the higher concentrations (around 10–20 μM) of fatty acids (Fig. S6). Interestingly, FB1 (with no quenching effect under the applied conditions; Fig. S6A), fatty acids, *N*-acyl-FB1 metabolites, and *O*-acyl-FB1 derivatives caused different changes in the emission signal of HSA. Based on the mycotoxin-induced increase in the fluorescence of the protein, we made an estimation regarding the stability of these mycotoxin–HSA complexes. Nevertheless, we did these calculations assuming 1:1 stoichiometry; while our earlier results suggested that acyl-FB1 derivatives may occupy more binding sites [11]. Considering the possibility of multiple binding sites, we tried to apply spectrum resolution and evaluations assuming other stoichiometries; however, we did not see that these can provide reliable data. In addition, if we hypothesize the presence of multiple binding sites for acyl-FB1 derivatives on HSA, then we should also consider the variable (e.g., increasing, decreasing, or even neutral) effects of the individual interactions on the emission signal of the protein, which makes the evaluation extremely difficult. Therefore, to provide more established data for the binding constants and the number of binding sites, mycotoxin–HSA interactions were also examined with ITC.

3.4. Interactions of acyl-FB1 derivatives with HSA based on isothermal titration calorimetry

In ITC experiments, HSA was titrated with increasing concentrations of the mycotoxins, where the heat effects of the dilution in the solvent were determined independently for each mycotoxin and then it was subtracted from the heat effects of the titration (Fig. S7). Calculated in such a way, the heat effects caused by the direct interactions of HSA with the mycotoxins were analyzed with multi-parameter non-linear regression using One Set of Sites model (see in Fig. 4 and Fig. S8), during which the stoichiometry, the binding constants, and the standard thermodynamic parameters were determined (Table 2).

Based on our results, 5-*O*-pal-FB1 and *N*-ole-FB1 likely occupy one binding site on the protein, while *N*-pal-FB1, 5-*O*-ole-FB1, *N*-lin-FB1, and 5-*O*-lin-FB1 may have three to four binding sites on HSA. The binding constants of each mycotoxin–HSA complex were higher than 10^5 L/mol (Table 2) indicating the formation of stable supramolecular complexes in a thermodynamically spontaneous manner ($\Delta G < 0$). In agreement with these data, fluorescence spectroscopic studies also recommended that the binding constants of mycotoxin–HSA complexes exceed 10^5 L/mol (see in

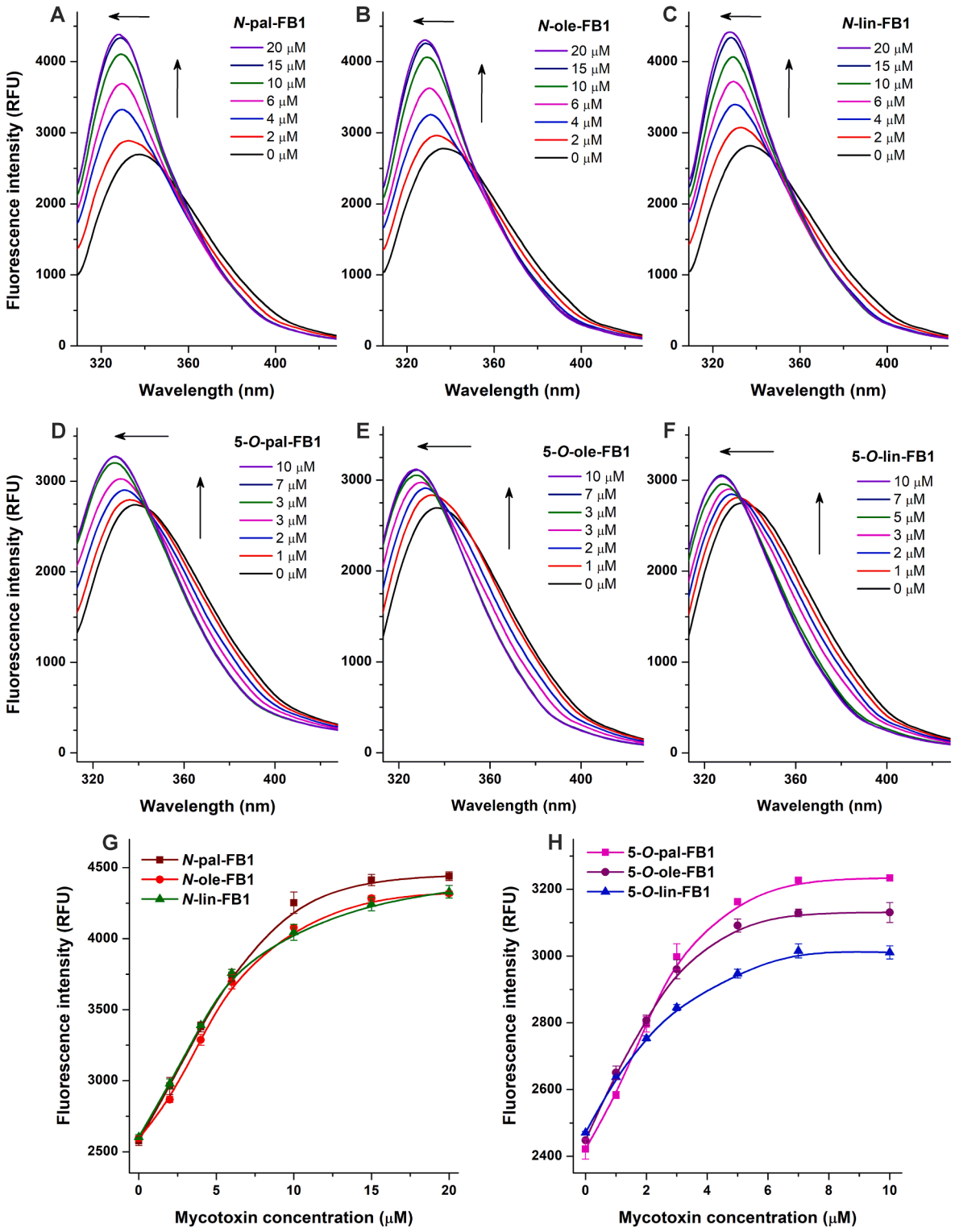

Fig. 3. Representative fluorescence emission spectra of HSA (2 μM) without and with *N*-acyl-FB1 (0–20 μM; panels **A**, **B**, and **C**) or 5-*O*-acyl-FB1 (0–10 μM; panels **D**, **E**, and **F**) derivatives in PBS (pH 7.4; $\lambda_{ex} = 295$ nm). Changes in the emission signal of HSA in the presence of increasing *N*-acyl-FB1 ($\lambda_{em} = 329$ nm; **G**) and 5-*O*-acyl-FB1 ($\lambda_{em} = 327$ nm; **H**) concentrations. Acyl-FB1 metabolites alone (without HSA) did not show emission signals at the wavelengths used.

Section 3.3). For all the six studied acyl-FB1 derivatives, the binding enthalpy was exothermic ($\Delta H < 0$), suggesting that their direct interaction with HSA dominates over the effects of the partial desolvation of the ligands and the protein. Binding of 5-*O*-pal-FB1 and *N*-ole-FB1 (with single binding site) is more exothermic compared to the other four mycotoxins studied.

N-ole-FB1 was the sole mycotoxin where we noticed a decrease in disordering ($\Delta S < 0$), suggesting conformational changes during the complex formation. The binding entropies of the other mycotoxins examined were positive ($\Delta S > 0$) and showed the increase in

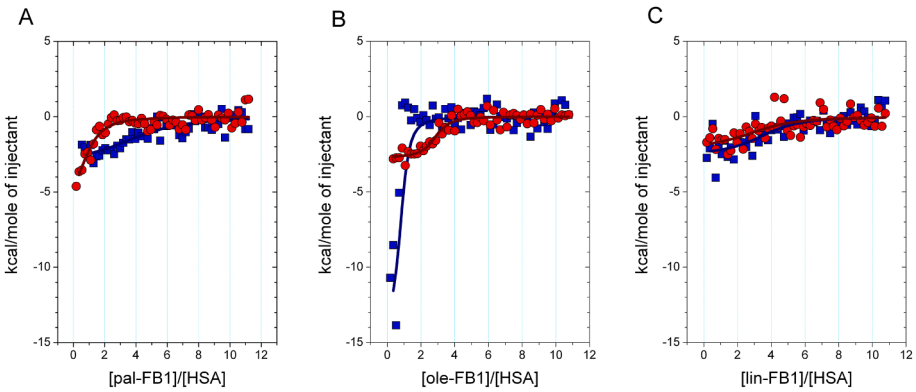

Fig. 4. Thermal effects of the direct interaction between HSA and mycotoxins, described with One Set of Sites model (solid lines) for *N*-pal-FB1 (**A**; blue squares), 5-*O*-pal-FB1 (**A**; red circles), *N*-ole-FB1(**B**; blue squares), 5-*O*-ole-FB1 (**B**; red circles), *N*-lin-FB1 (**C**; blue squares), and 5-*O*-lin-FB1 (**C**; red circles).

Table 2
Stoichiometric parameters (n), decimal logarithmic values of the binding constants (log$K$; where the unit of K is L/mol), and standard thermodynamic parameters (enthalpy, ΔH; entropy, ΔS; and Gibbs free energy, ΔG) of the mycotoxin–HSA complexes examined.

Mycotoxin	n	log$K$	ΔH [kcal mol^{-1}]	ΔS [cal K^{-1} mol^{-1}]	ΔG [kcal mol^{-1}]
N-pal-FB1	3.5 ± 0.8	5.38 ± 0.19	−3.20 ± 0.60	13.9 ± 2.8	−7.34 ± 0.25
5-*O*-pal-FB1	0.9 ± 0.5	5.66 ± 0.30	−6.54 ± 0.40	4.0 ± 2.5	−7.72 ± 0.36
N-ole-FB1	0.8 ± 0.2	6.38 ± 0.20	−14.0 ± 2.2	−17.8 ± 8.3	−8.70 ± 0.26
5-*O*-ole-FB1	2.8 ± 0.3	6.45 ± 0.26	−2.74 ± 0.18	20.3 ± 1.7	−8.80 ± 0.32
N-lin-FB1	3.8 ± 0.5	5.73 ± 0.50	−2.56 ± 0.46	17.6 ± 3.2	−7.81 ± 0.49
5-*O*-lin-FB1	3.5 ± 0.8	5.54 ± 0.45	−2.12 ± 0.66	18.3 ± 3.8	−7.56 ± 0.46

disordering during the association (Table 2). Furthermore, the entropy values of *N*-pal-FB1, 5-*O*-ole-FB1, *N*-lin-FB1, and 5-*O*-lin-FB1 (with three to four binding sites on HSA) were higher compared to the binding entropy of 5-*O*-pal-FB1 (one binding site on the protein), which may reflect the release of more solvent molecules during the partial desolvation of the binding sites.

Fatty acids have nine typical binding sites (FA1–FA9) in HSA; among these, drugs and other xenobiotics most frequently occupy FA7 (Sudlow's Site I, in subdomain IIA) or FA3–FA4 (Sudlow's Site II, in subdomain IIIA) [43,44]. The high-affinity interaction of fatty acids with HSA is well-known for decades [43,45–47]. Therefore, it was reasonable to assume the strong interactions of acyl-FB1 derivatives with HSA, while it was unlikely that the relatively hydrophilic FB1 could form highly stable complexes with the protein. In agreement with this hypothesis, we observed only weak interaction of FB1 with HSA (log$K$ = 3.2) [11], while acyl-FB1 derivatives bound to the protein with very high affinity (Table 2). Serum albumin is the most abundant plasma protein in the blood; besides its other important physiological roles, it can bind and carry numerous ligands in the circulation [43]. Therefore, the formation of stable ligand–albumin complexes can be high pharmacological and/or toxicological importance [44]. The high affinity interactions of acyl-FB1 compounds with HSA suggest that these ligands appear dominantly in albumin-bound form in the circulation. The strong albumin binding of ligands in the circulation can cause a depot effect [43]: the partial entrapment in the intravascular water space can result in slower tissue distribution and/or elimination of these compounds. Nevertheless, we need to emphasize that several other factors can influence the toxicokinetic and toxicodynamic properties of xenobiotics; therefore, we would like to avoid drawing further, speculative conclusions. Additional *in vivo* studies are reasonable in the future to understand the toxicological importance of acyl-FB1–albumin interactions, including the possible species-dependent variations.

3.5. Effects of acyl-FB1 derivatives on the albumin binding of Sudlow's site I and site II markers

In ultrafiltration experiments, the unbound site marker molecules can pass through the filter (30 kDa), while HSA and albumin-bound molecules are retained. Therefore, the elevated level of the site marker in the filtrate demonstrates its displacement or its reduced binding affinity, while the decreased concentration of the site marker in the filtrate indicates its stronger interaction with the protein [23,26]. In our earlier report, using the same experimental models, we demonstrated that FB1 does not affect the albumin binding of warfarin (Site I) and naproxen (Site II), which is in agreement with its low binding affinity (log$K$ = 3.2) [11].

Based on the previous measurements with palmitic acid and palmitoyl-FB1 derivatives [11] as well as our current experiments with oleic acid, linoleic acid, oleoyl-FB1 and linoleoyl-FB1 metabolites (Fig. 5A), we can summarize the following observations regarding their effects on the albumin binding of warfarin. Palmitic acid, oleic acid, and linoleic acid significantly decreased the filtered fraction of warfarin, suggesting that fatty acids stabilize the warfarin–HSA complex. It is in agreement with earlier studies which also demonstrated that fatty acids increase the binding affinity of warfarin towards HSA [23,48]. In contrast, both *N*-acyl- and 5-*O*-acyl-FB1 metabolites strongly increased the concentrations of warfarin in the filtrate (Fig. 5A), indicating the considerably elevated free fraction of the Site I marker. Thus, each acyl-FB1 metabolite tested can disrupt warfarin–HSA interaction, where *N*-acyl derivatives showed somewhat stronger or similar impacts compared to the 5-*O*-acyl compounds.

The effects of fatty acids and acyl-FB1 derivatives on the albumin binding of naproxen were also examined. Fatty acids and *N*-acyl metabolites considerably increased the filtered fraction of naproxen, indicating marked decreases in the albumin binding of the Site II marker (Fig. 5B). Thus, these compounds can strongly disrupt naproxen–HSA interaction. However, our previous [11] and

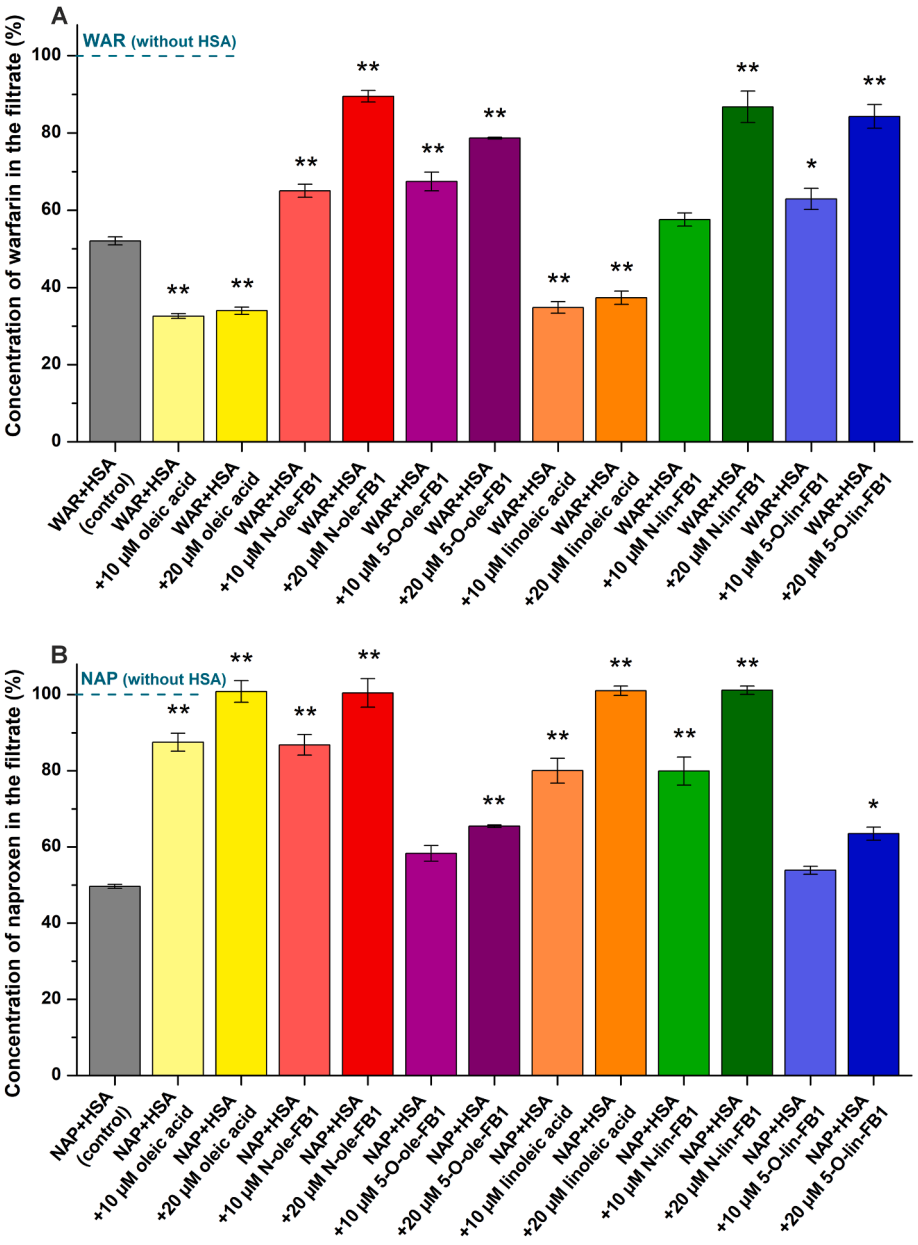

Fig. 5. Effects of oleic acid, *N*-ole-FB1, 5-*O*-ole-FB1, linoleic acid, *N*-lin-FB1 and 5-*O*-lin-FB1 on the filtered concentrations of the Sudlow's Site I marker warfarin (WAR; **A**) and the Sudlow's Site II marker naproxen (NAP; **B**). Before ultrafiltration, samples contained WAR + HSA (1.0 μM and 5.0 μM, respectively) or NAP + HSA (1.0 μM and 1.5 μM, respectively) without or with the ligands tested (0, 10, and 20 μM) in PBS (pH 7.4). In both assays, 100 % means the level of the site marker in the filtrate when the site marker was filtered alone (without the protein; marked with cyan dashed lines). Effects of FB1, palmitic acid, *N*-pal-FB1 and 5-*O*-ole-FB1 in the same experimental models are presented in our earlier report [11].

current data (Fig. 5B) highlighted that *O*-acyl-FB1 derivatives can cause no or only minor displacement of naproxen from HSA.

Similar to fluorescence quenching experiments (Fig. 3), ultrafiltration studies (Fig. 5) denote that fatty acids, *N*-acyl-FB1 metabolites, and 5-*O*-acyl-FB1 derivatives can behave differently, which may be resulted from some discrepancies in their binding sites and/or binding positions. These data suggest that the site of acylation (*N*-acyl or 5-*O*-acyl) may have higher importance than the structure of the fatty acid which acylates the mycotoxin. On the other hand, ITC measurements demonstrated that the binding affinities and the number of binding sites are strongly influenced by the fatty acid component presented (Table 2), which underlines the complexity of these interactions. Based on ultrafiltration experiments, *N*-acyl derivatives can strongly displace both Site II and Site I ligands (Fig. 5B), suggesting their possibly similar binding sites/positions on HSA. Modeling studies suggested that *N*-pal-FB1 may have binding sites at both of these regions [11]. Nevertheless, we cannot be sure that the increased free fractions of the site markers noticed are caused by direct displacement or by allosteric modulation. Despite that modeling studies recommended Site II as the binding site of 5-*O*-pal-FB1 on HSA [11], 5-*O*-acyl metabolites had no or only minor effects on the albumin binding of naproxen. Therefore, 5-*O*-acyl-FB1 derivatives likely have no high-affinity binding site on Site II; while they may occupy Site I or a region near to this binding site, based on their strong impacts on the albumin binding of warfarin (Fig. 5A).

4. Conclusions

In this study, we examined the toxic effects of acyl-FB1 derivatives on zebrafish embryos and their interactions with HSA. Based on both the mortality data and the mycotoxin-induced sublethal malformations, acyl-FB1 metabolites exerted much stronger toxicity than FB1. Furthermore, *N*-acyl compounds proved to be more toxic compared to the 5-*O*-acyl derivatives. After 120 h exposure, low micromolar levels of *N*-pal-FB1 and *N*-ole-FB1 caused significant mortality in zebrafish embryos. Nevertheless, *N*-pal-FB1 showed marked impacts even after 24 h, while the toxic effects of *N*-ole-FB1 was gradually increased during the 5 days of exposure. Both fluorescence spectroscopic and ITC measurements demonstrated the strong interactions of acyl-FB1 metabolites with HSA. 5-*O*-pal-FB1 and *N*-ole-FB1 likely occupy one binding site on HSA, while *N*-pal-FB1, 5-*O*-ole-FB1, *N*-lin-FB1, and 5-*O*-lin-FB1 may have three to four binding sites. The very limited data available in regard to the formation and occurrence of acyl-FB1 compounds do not make possible a proper estimation of their intake. Nevertheless, *N*-acyl-FB1 derivatives can appear as food contaminants and are also formed *in vivo* after the exposure to FB1. In addition, the toxic potency of *N*-acyl-FB1 metabolites remarkably higher compared to FB1 and it even higher vs. 5-*O*-acyl-FB1 derivatives. Therefore, it is reasonable the hypothesize the significant toxicological importance of the *N*-acyl-FB1 compounds. Nevertheless, further extensive studies are required to collect more data in regard to the occurrence, the toxicokinetics, and the toxic effects of acyl-FB1 metabolites.

CRediT authorship contribution statement

Zsolt Csenki: Writing – original draft, Validation, Supervision, Methodology, Funding acquisition. **Illés Bock:** Writing – original draft, Investigation, Formal analysis. **Levente Horváth:** Resources. **Artur Stepniak:** Investigation, Formal analysis. **Béla Fiser:** Writing – original draft, Validation, Supervision, Investigation, Formal analysis. **Adam Buczkowski:** Investigation, Formal analysis. **Gergő Tóth:** Validation, Funding acquisition. **Dávid Csabai:** Investigation, Formal analysis. **Dávid Hesszenberger:** Investigation, Formal analysis. **Anikó Lajtai:** Validation, Supervision. **Sándor Kunsági-Máté:** Writing – original draft, Validation, Funding acquisition, Formal analysis. **Melinda Kovács:** Funding acquisition, Conceptualization. **István Szabó:** Resources, Funding acquisition. **Balázs Kriszt:** Resources, Conceptualization. **Tibor Bartók:** Validation, Supervision, Resources, Methodology. **Miklós Poór:** Writing – original draft, Validation, Supervision, Methodology, Investigation, Funding acquisition, Formal analysis, Conceptualization.

Declaration of competing interest

The authors declare the following financial interests/personal relationships which may be considered as potential competing interests: Authors Levente Horváth and Tibor Bartók are employed by the company Fumizol Ltd. They prepared, purified, and provided FB1 and acyl-FB1 derivatives for the investigations described in the current study; however, Levente Horváth and Tibor Bartók had no involvement in the design of the study as well as in the collection, analyses, or interpretation of the data presented. The remaining authors declare no competing financial interest. If there are other authors, they declare that they have no known competing financial interests or personal relationships that could have appeared to influence the work reported in this paper.

Acknowledgements

The work of M.P. was supported by the Hungarian National Research, Development and Innovation Office (FK 138184). This research was also financed by the Research Excellence Programme (Z.C.) and the Flagship Research Groups Programme (I.S.) of the Hungarian University of Agriculture and Life Sciences. The work of I.B. was supported by the EKÖ P-MATE/2024/25/K University Research Scholarship Program of the Ministry for Culture and Innovation from the source of the National Research, Development and Innovation Fund. This research was funded by the Hungarian Ministry for Innovation and Technology Project no. TKP2021-EGA-17 (S.K-M.). This work was funded by the National Research, Development, and Innovation Office, Hungary (grant: NKFIH, FK 146930) and supported by the Já nos Bolyai Research Scholarship of the Hungarian Academy of Sciences (G.T.). The support of the Hungarian National Laboratory project RRF-2.3.1-21-2022-00007 is gratefully acknowledged (M.K.).

Appendix A. Supplementary data

Supplementary data to this article can be found online at https://doi.org/10.1016/j.emcon.2025.100620.

References

[1] Z.E. Martins, H. Ramos, A.M. Araújo, M. Silva, M. Ribeiro, A. Melo, C. Mansilha, O. Viegas, M.A. Faria, I.M.P.L.V.O. Ferreira, From data to insight: exploring contaminants in different food groups with literature mining and machine learning techniques, Curr. Res. Food Sci. 7 (2023) 100557, https://doi.org/10.1016/j.crfs.2023.100557.

[2] H.K. Knutsen, J. Alexander, L. Barregård, M. Bignami, B. Brüschweiler, S. Ceccatelli, B. Cottrill, M. Dinovi, L. Edler, B. Grasl-Kraupp, et al., Risks for animal health related to the presence of fumonisins, their modified forms and hidden forms in feed, EFSA J. 16 (2018) e05242, https://doi.org/10.2903/j.efsa.2018.5242.

[3] J.P. Rheeder, W.F.O. Marasas, H.F. Vismer, Production of fumonisin analogs by fusarium species, Appl. Environ. Microbiol. 68 (2002) 2101–2105, https://doi.org/10.1128/AEM.68.5.2101-2105.2002.

[4] J.C. Frisvad, J. Smedsgaard, R.A. Samson, T.O. Larsen, U. Thrane, Fumonisin B 2 production by Aspergillus Niger, J. Agric. Food Chem. 55 (2007) 9727–9732, https://doi.org/10.1021/jf0718906.

[5] J.M. Mogensen, K.A. Møller, P. Von Freiesleben, R. Labuda, E. Varga, M. Sulyok, A. Kubátová, U. Thrane, B. Andersen, K.F. Nielsen, Production of fumonisins B2 and B4 in tolypocladium species, J. Ind. Microbiol. Biotechnol. 38 (2011) 1329–1335, https://doi.org/10.1007/s10295-010-0916-1.

[6] Z. Gao, K. Luo, Q. Zhu, J. Peng, C. Liu, X. Wang, S. Li, H. Zhang, The natural occurrence, toxicity mechanisms and management strategies of fumonisin B1:A review, Environ. Pollut. 320 (2023) 121065, https://doi.org/10.1016/j.envpol.2023.121065.

[7] A. Anttila, R.V. Bhat, J.A. Bond, S.J. Borghoff, F.X. Bosch, G.P. Carlson, M. Castegnaro, G. Cruzan, W.C.A. Gelderblom, U. Hass, et al., IARC monographs on the evaluation of carcinogenic risks to humans: some traditional herbal medicines, some mycotoxins, naphthalene and styrene, IARC (Int. Agency Res. Cancer) Monogr. Eval. Carcinog. Risks Hum. 82 (2002) i-vi+1-551. https://publications.iarc.who.int/Book-And-Report-Series/Iarc-Monographs-On-The-Identification-Of-Carcinogenic-Hazards-To-Humans/Some-Traditional-Herbal-Medicines-Some-Mycotoxins-Naphthalene-And-Styrene-2002.

[8] K. Hu, Y. Cao, Ping, pong, and freeze: structural insights into the inhibition of ceramide synthase by fumonisin B1, Structure 32 (2024) 1296–1298, https://doi.org/10.1016/j.str.2024.08.010.

[9] M. Bryła, M. Roszko, K. Szymczyk, R. Jedrzejczak, M.W. Obiedziński, Fumonisins and their masked forms in maize products, Food Control 59 (2016) 619–627, https://doi.org/10.1016/j.foodcont.2015.06.032.

[10] H. Harrer, E.L. Laviad, H.U. Humpf, A.H. Futerman, Identification of N-acyl-fumonisin B1 as new cytotoxic metabolites of fumonisin mycotoxins, Mol. Nutr. Food Res. 57 (2013) 516–522, https://doi.org/10.1002/mnfr.201200465.

[11] Z. Csenki, T. Bartók, I. Bock, L. Horváth, B. Lemli, B.Z. Zsidó, C. Angeli, C. Hetényi, I. Szabó, B. Urbányi, et al., Interaction of fumonisin B1, N-Palmitoyl-Fumonisin B1, 5-O-Palmitoyl-Fumonisin B1, and fumonisin B4 mycotoxins with human serum albumin and their toxic impacts on zebrafish embryos, Biomolecules 13 (2023) 755, https://doi.org/10.3390/biom13050755.

[12] H.K. Knutsen, L. Barregård, M. Bignami, B. Brüschweiler, S. Ceccatelli, B. Cottrill, M. Dinovi, L. Edler, B. Grasl-Kraupp, C. Hogstrand, et al., Appropriateness to set a group health-based guidance value for fumonisins and

their modified forms, EFSA J. 16 (2018) e05172, https://doi.org/10.2903/j.efsa.2018.5172.
[13] C. Angeli, T.M. Nagy, L. Horváth, M. Varga, A. Szekeres, G.K. Tóth, T. Janáky, J. Szolomájer, M. Kovács, K.E. Kövér, et al., Preparation of 3-O-, 5-O- and N-palmitoyl derivatives of fumonisin B1 toxin and their characterisation with NMR and LC-HRMS methods, Food Addit. Contam. 39 (2022) 1759–1771, https://doi.org/10.1080/19440049.2022.2116112.
[14] W.T. Shier, H.K. Abbas, M. Abou-Karam, F.A. Badria, P.A. Resch, Fumonisins: abiogenic conversions of an environmental tumor promoter and common food contaminant, J. Toxicol. - Toxin Rev. 22 (2003) 591–616, https://doi.org/10.1081/TXR-120026916.
[15] T. Bartók, Á. Szécsi, K. Juhász, M. Bartók, Á. Mesterházy, ESI-MS and MS/MS identification of the first ceramide analogues of fumonisin B1 mycotoxin from a Fusarium verticillioides culture following RP-HPLC separation, Food Addit. Contam. 30 (2013) 1651–1659, https://doi.org/10.1080/19440049.2013.809626.
[16] H. Harrer, H.U. Humpf, K.A. Voss, In vivo formation of N-acyl-fumonisin B1, Mycotoxin Res. 31 (2015) 33–40, https://doi.org/10.1007/s12550-014-0211-5.
[17] Z. Zhang, Q. Fang, T. Xie, X. Gong, Mechanism of ceramide synthase inhibition by fumonisin B1, Structure 32 (2024) 1419–1428, https://doi.org/10.1016/j.str.2024.06.002.
[18] F. Perugino, L. Pedroni, G. Galaverna, C. Dall'Asta, L. Dellafiora, Grasping the duality of fumonisins versus ceramide synthases: a computational approach to study their role as inhibitors and substrates from a mechanistic standpoint, Heliyon 11 (2025) e43725, https://doi.org/10.1016/j.heliyon.2025.e43725.
[19] T. Bartók, L. Tölgyesi, Á. Mesterházy, M. Bartók, Á. Szécsi, Identification of the first fumonisin mycotoxins with three acyl groups by ESI-ITMS and ESI-TOFMS following RP-HPLC separation: palmitoyl, linoleoyl and oleoyl EFB1 fumonisin isomers from a solid culture of Fusarium verticillioides, Food Addit. Contam. 27 (2010) 1714–1723, https://doi.org/10.1080/19440049.2010.521958.
[20] C. Falavigna, I. Lazzaro, G. Galaverna, P. Battilani, C. Dall'Asta, Fatty acid esters of fumonisins: first evidence of their presence in maize, Food Addit. Contam. 30 (2013) 1606–1613, https://doi.org/10.1080/19440049.2013.802839.
[21] C. Falavigna, I. Lazzaro, G. Galaverna, C. Dall'Asta, P. Battilani, Oleoyl and linoleoyl esters of fumonisin B1 are differently produced by Fusarium verticillioides on maize and rice based media, Int. J. Food Microbiol. 217 (2016) 79–84, https://doi.org/10.1016/j.ijfoodmicro.2015.10.013.
[22] M. Haq, N. Gonzalez, K. Mintz, A. Jaja-Chimedza, C.L. De Jesus, C. Lydon, A. Welch, J.P. Berry, Teratogenicity of ochratoxin a and the degradation product, ochratoxin α, in the zebrafish (Danio rerio) embryo model of vertebrate development, Toxins 8 (2016) 40, https://doi.org/10.3390/toxins8020040.
[23] B. Lemli, Z. Lomozová, T. Huber, A. Lukács, M. Poór, Effects of heme site (FA1) ligands bilirubin, biliverdin, hemin, and methyl Orange on the albumin binding of site I marker warfarin: complex allosteric interactions, Int. J. Mol. Sci. 23 (2022) 14007, https://doi.org/10.3390/ijms232214007.
[24] B. Lemli, P. Vilmányi, E. Fliszár-Nyúl, B.Z. Zsidó, C. Hetényi, L. Szente, M. Poór, Testing serum albumins and cyclodextrins as potential binders of the mycotoxin metabolites Alternariol-3-Sulfate, Alternariol-9-Monomethylether and Alternariol-9-Monomethylether-3-Sulfate, Int. J. Mol. Sci. 23 (2022) 14353, https://doi.org/10.3390/ijms232214353.
[25] V. Mohos, E. Fliszár-Nyúl, G. Schilli, C. Hetényi, B. Lemli, S. Kunsági-Máté, B. Bognár, M. Poór, Interaction of chrysin and its main conjugated metabolites chrysin-7-sulfate and chrysin-7-glucuronide with serum albumin, Int. J. Mol. Sci. 19 (2018) 4073, https://doi.org/10.3390/ijms19124073.
[26] E. Fliszár-Nyúl, B. Lemli, S. Kunsági-Máté, L. Dellafiora, C. Dall'Asta, G. Cruciani, G. Pethő, M. Poór, Interaction of mycotoxin alternariol with serum albumin, Int. J. Mol. Sci. 20 (2019) 2352, https://doi.org/10.3390/ijms20092352.
[27] B. du Plessis, T. Regnier, S. Combrinck, P. Heinrich, T. Braunbeck, Effect of pH on the toxicity of fumonisins towards the RTL-W1 cell line and zebrafish (Danio rerio) embryos, Toxicol. Lett. 313 (2019) 101–107, https://doi.org/10.1016/j.toxlet.2019.06.009.
[28] N.A. Ducharme, L.E. Peterson, E. Benfenati, D. Reif, C.W. McCollum, J.T. Gustafsson, M. Bondesson, Meta-analysis of toxicity and teratogenicity of 133 chemicals from zebrafish developmental toxicity studies, Reprod. Toxicol. 41 (2013) 98–108, https://doi.org/10.1016/j.reprotox.2013.06.070.
[29] C. Lumsangkul, H.I. Chiang, N.W. Lo, Y.K. Fan, J.C. Ju, Developmental toxicity of mycotoxin fumonisin B 1 in animal embryogenesis: an overview, Toxins 11 (2019) 114, https://doi.org/10.3390/toxins11020114.
[30] W.F.O. Marasas, R.T. Riley, K.A. Hendricks, V.L. Stevens, T.W. Sadler, J. Gelineau-van Waes, S.A. Missmer, J. Cabrera, O. Torres, W.C.A. Gelderblom, et al., Fumonisins disrupt sphingolipid metabolism, folate transport, and neural tube development in embryo culture and in vivo: a potential risk factor for human neural tube defects among populations consuming fumonisin-contaminated maize, J. Nutr. 134 (2004) 711–716, https://doi.org/10.1093/jn/134.4.711.
[31] A.L. Rubinstein, Zebrafish assays for drug toxicity screening, Expet Opin. Drug Metabol. Toxicol. 2 (2006) 231–240, https://doi.org/10.1517/17425255.2.2.231.
[32] C. De Esch, R. Slieker, A. Wolterbeek, R. Woutersen, D. de Groot, Zebrafish as potential model for developmental neurotoxicity testing. A mini review, Neurotoxicol. Teratol. 34 (2012) 545–553, https://doi.org/10.1016/j.ntt.2012.08.006.
[33] A. Juan-García, M.A. Bind, F. Engert, Larval zebrafish as an in vitro model for evaluating toxicological effects of mycotoxins, Ecotoxicol. Environ. Saf. 202 (2020) 110909, https://doi.org/10.1016/j.ecoenv.2020.110909.
[34] G. Yang, Y. Wang, T. Wang, D. Wang, H. Weng, Q. Wang, C. Chen, Variations of enzymatic activity and gene expression in zebrafish (Danio rerio) embryos co-exposed to zearalenone and fumonisin B1, Ecotoxicol. Environ. Saf. 222 (2021) 112533, https://doi.org/10.1016/j.ecoenv.2021.112533.
[35] S. Scholz, S. Fischer, U. Gündel, E. Küster, T. Luckenbach, D. Voelker, The zebrafish embryo model in environmental risk assessment - applications beyond acute toxicity testing, Environ. Sci. Pollut. Control Ser. 15 (2008) 394–404, https://doi.org/10.1007/s11356-008-0018-z.
[36] S. Weigt, N. Huebler, R. Strecker, T. Braunbeck, T.H. Broschard, Zebrafish (Danio rerio) embryos as a model for testing proteratogens, Toxicology 281 (2011) 25–36, https://doi.org/10.1016/j.tox.2011.01.004.
[37] I.W.T. Selderslaghs, A.R. Van Rompay, W. De Coen, H.E. Witters, Development of a screening assay to identify teratogenic and embryotoxic chemicals using the zebrafish embryo, Reprod. Toxicol. 28 (2009) 308–320, https://doi.org/10.1016/j.reprotox.2009.05.004.
[38] H. Stockmann-Juvala, K. Savolainen, A review of the toxic effects and mechanisms of action of fumonisin B 1, Hum. Exp. Toxicol. 27 (2008) 799–809, https://doi.org/10.1177/0960327108099525.
[39] J.H. He, S.Y. Guo, F. Zhu, J.J. Zhu, Y.X. Chen, C.J. Huang, J.M. Gao, Q.X. Dong, Y.X. Xuan, C.Q. Li, A zebrafish phenotypic assay for assessing drug-induced hepatotoxicity, J. Pharmacol. Toxicol. Methods 67 (2013) 25–32, https://doi.org/10.1016/j.vascn.2012.10.003.
[40] R. van den Boom, L. Vergauwen, D. Knapen, Effects of metabolic disruption on lipid metabolism and yolk retention in zebrafish embryos, Environ. Toxicol. Chem. 43 (2024) 1880–1893, https://doi.org/10.1002/etc.5930.
[41] L. Wang, C. Liang, N. Zheng, C. Yang, S. Yan, X. Wang, Z. Zuo, C. He, Kidney injury contributes to edema of zebrafish larvae caused by quantum dots, Sci. Total Environ. 908 (2024) 168420, https://doi.org/10.1016/j.scitotenv.2023.168420.
[42] L. Mátyus, J. Szöllosi, A. Jenei, Steady-state fluorescence quenching applications for studying protein structure and dynamics, J. Photochem. Photobiol. B Biol. 83 (2006) 223–236, https://doi.org/10.1016/j.jphotobiol.2005.12.017.
[43] G. Fanali, A. Di Masi, V. Trezza, M. Marino, M. Fasano, P. Ascenzi, Human serum albumin: from bench to bedside, Mol. Aspect. Med. 33 (2012) 209–290, https://doi.org/10.1016/j.mam.2011.12.002.
[44] K. Yamasaki, V.T.G. Chuang, T. Maruyama, M. Otagiri, Albumin-drug interaction and its clinical implication, Biochim. Biophys. Acta, Gen. Subj. 1830 (2013) 5435–5443, https://doi.org/10.1016/j.bbagen.2013.05.005.
[45] S. Curry, H. Mandelkow, P. Brick, N. Franks, Crystal structure of human serum albumin complexed with fatty acid reveals an asymmetric distribution of binding sites, Nat. Struct. Biol. 5 (1998) 827–835, https://doi.org/10.1038/1869.
[46] J.A. Hamilton, NMR reveals molecular interactions and dynamics of fatty acid binding to albumin, Biochim. Biophys. Acta, Gen. Subj. 1830 (2013) 5418–5426, https://doi.org/10.1016/j.bbagen.2013.08.002.
[47] G.V. Richieri, A. Anel, A.M. Kleinfeld, Interactions of long-chain fatty acids and albumin: determination of free fatty acid levels using the fluorescent probe ADIFAB, Biochemistry 32 (1993) 7574–7580, https://doi.org/10.1021/bi00080a032.
[48] H. Vorum, B. Honoré, Influence of fatty acids on the binding of warfarin and phenprocoumon to human serum albumin with relation to anticoagulant therapy, J. Pharm. Pharmacol. 48 (1996) 870–875, https://doi.org/10.1111/j.2042-7158.1996.tb03990.x.